SERBIAN JOURNAL OF ELECTRICAL ENGINEERING
Vol. 19, No. 1, February 2022, 1-14
UDC: 621.314.1:620.92 **DOI: https://doi.org/10.2298/SJEE2201001H**

High Voltage Gain Resonant DC-DC Converter with VM Cells for Renewable Sources Applications

Saeed Hasanzadeh[1], Seyed Mohsen Salehi[1], Ehsan Najafi [1], Farinaz Horri[1]

Abstract: Due to the widespread impact of renewable energy resources on high power density grids, transmission at the DC regime has been considered more useful than AC transmission systems. The findings of this study suggest the application of a ripple-free input current resonant DC-DC converter possessing high voltage gain and high efficiency as being more suitable for renewable energy systems. Applying variable switching frequency control systems, the proposed converter discussed here is generally operated at the critical conduction mode for soft switching of the semiconductor switches. Using the resonance mechanism, the proposed converter causes a decrease in the turn-on loss of the power switch without needing additional semiconductor gadgets. It leads to a reduction in the reverse-recovery losses of the rectifying diodes. Also, analysis and design consideration of the proposed converter are presented with excellent performance.

Keywords: Resonant DC-DC Converter, Renewable Energy, Voltage Multiplier.

1 Introduction

In the past decades, high efficiency with high power density, simple structure, and fast DC-DC converters have been employed for high power density electrical applications [1]. A pulse width modulation (PWM) control is generally used in the DC-DC converters. Due to the hard switching of these converters, increasing the switching frequency for small size, the switching losses associated with the on and off states of the semiconductor components of the DC-DC converter increase (MOSFET on losses and diode off losses). These losses are so significant that the operations of the converter limit in the high frequency [2]. PSOL and Super lift DC-DC converters may find high voltage gain. But still, they suffer from hard switching losses [3, 4]. Several full, quasi, and multi-resonant DC-DC converters have been proposed in the literature to solve these problems. Nevertheless, resonant converters have been shown to attain low switching losses at high frequencies than PWM converters, and their passive components have small sizes due to high switching frequency [5]. However, these converters have

[1]Department of Electrical and Computer Engineering, Qom University of Technology, Qom, Iran
E-mails: hasanzadeh@qut.ac.ir; sm.salehi3@gmail.com; najafi@qut.ac.ir; farinazhori90@gmail.com

some limitations, including complexity, electromagnetic interference (EMI), and input/output filter design because various switching frequencies are required to control the output voltage.

The hard-switching DC-DC converters are usually under major stresses caused by high peak voltages and currents. Several isolated DC-DC converters have achieved a high boost conversion ratio through the increase in the turn ratio of the coupled inductors. Forward and flyback topologies are supposed to be the most appealing converters among other structures due to their simple control systems and circuits [6 , 7]. Nonetheless, they suffer from high switching loss due to their leakage inductance and reverse recovery energy of diodes which compromise their efficiency [8]. To overcome the shortcomings, Forward and flyback converters with an active or passive clamp circuit were suggested [9]. The problem is solved by recycling the leakage inductance energy in the related research. In addition, all switches achieve zero voltage switching while turning on.

Moreover, the clamp circuit maintains a constant voltage across the switches. Consequently, a number of active clamp DC-DC topologies were developed [10, 11]. Although the conventional DC-DC topologies transfer power to the output load only when their switch is on or off, the coupled inductor structures can transfer energy at all states regardless of the switching conditions [10 – 13]. A two-stage converter with a resonant inverter cascaded with a rectifier to increase the voltage gain is also proposed [14]. Therefore, the switching loss decreases due to the resonant converter's soft switching. Resonance phenomena enable converters to have high frequency switching, increasing the converter's control system bandwidth, power density, and reduction in overall sizing [13, 14]. Connecting the rectifiers' multiple outputs in series can also culminate in high voltage gain [15]. However, the method is solely utilized in applications, their isolations between input’s and output’s ground. For the topology proposed in [15] the DC-AC stage mainly achieves the voltage ratio conversation. Moreover, the AC-DC stage attains little voltage gain. The problem is solved in [16]. The voltage gain is high, using interleave technique. Although, a large number of components is one of the disadvantages of this converter.

Conversely, some circuits [12 – 14] are operational in the condition that the AC-DC stage mainly attains the voltage gain. There are some demerits related to these methods, too. For example, a large number of capacitors are required if the AC-DC voltage gain is required. In addition, the overall efficiency of the converter will be decreased provided that DC/AC voltage gain increases due to the extra loss in inductors. [12 – 14]. Thus, one should strike a balance between voltage gains of different stages to improve overall circuit performance such as cost, efficiency, etc.

Moreover, the output voltage is directly proportional to the AC-DC peak output voltage [12 – 14]. In [17], a family of current-fed interleaved high step-up DC-DC converters has been proposed. In this paper, all semiconductor devices work under soft-switching situations. The high voltage gain and soft switching were achieved using the voltage multiplier circuit and the active clamp. High voltage gain, suitable efficiency, low ripple input current, and output voltage make it suitable for many applications [17].

The present study proposes a high voltage gain resonant DC-DC converter with ripple-free input current and high efficiency, suitable for renewable energy applications. A mechanism for switching and an input-current doubler are utilized to achieve considerable voltage gain with transformers having a low turns ratio. Its active clamp mechanism limits the voltage spikes across the semiconductor devices and recycles the transformer leakage inductance energy. In this paper, a converter is suggested that uses a resonance mechanism to greatly reduce switching losses.

2 Proposed Converter

The circuit diagram of the proposed converter is depicted in Fig. 1.

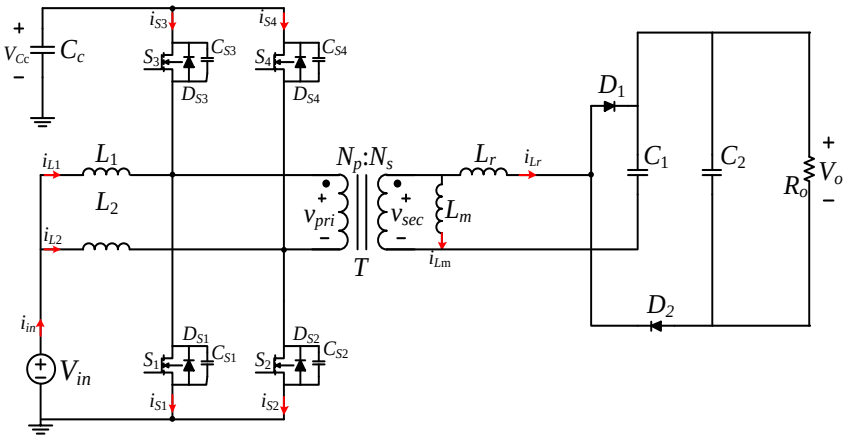

Fig. 1 – *The power circuit configuration of the proposed converter.*

The power components used in the proposed structure are:

1. The *i*-th MOSFET comprises an ideal switch S_i, a fast diode D_{Si} and a junction capacitor C_{Si}.
2. The diodes D_1 and D_2 as ideal diodes.
3. The capacitance of the capacitors C_1, C_2, and clamp capacitor (C_C) are comparatively high to keep their voltage almost constant.

4. The magnetizing current is approximately zero due to the large value of the magnetizing inductance L_m. Consequently, the transformer is only modeled with an ideal transformer and series inductor L_r.
5. As the inductance of the input inductors, L_1 and L_2 are equal, $L_1 = L_2 = L$.
6. The average input current, I_{in}, is divided identically between inductors; hence $I_{L1} = I_{L2} = I_L = I_{in}/2$, while the input current is i_{in}.

3 Analysis of the Proposed Structure

Equivalent circuits for the different intervals are as follows: **(a)** Mode 1: interval (t_0, t_1); **(b)** Mode 2: interval (t_1, t_2); **(c)** Mode 3: interval $(t_2, t_3 = T_s/2)$; **(d)** Mode 4: interval $(t_3 = T_s/2, t_4)$; **(e)** Mode 5: interval (t_4, t_5) and **(f)** Mode 6: interval $(t_5, t_6 = T)$.

Mode 1 (t_0, t_1): During this mode, the switches S_1, S_4 are turned on. Especially, S_4 is getting turn-on with ZVS because D_{S4} has been conducting in the previous mode. Diode D_2 current i_{D2} continues to flow in the same direction as before until it reaches zero. i_{L1} flows into S_1 and increases linearly as

$$i_{L1}(t) = i_{L1}(t_0) + \frac{V_{in}}{L_1}(t_0) \tag{1}$$

and i_{L2} decreases linearly as

$$i_{L2}(t) = i_{L2}(t_0) - \frac{V_{Cc} - V_{in}}{L_2}(t - t_0). \tag{2}$$

In this mode, the v_{sec} becomes

$$v_{sec}(t_0) = -nV_{Cc}. \tag{3}$$

Mode 2 (t_1, t_2): At time t_1, Diode D_2 is in forwarding bias, and Diode D_1 is in reversed bias. i_{L1} increases as (1), and i_{L2} decreases as (2). Capacitor C_2 is charged by Capacitor C_1 and the input power supply.

$$V_o = V_{C2}, \tag{4}$$

$$Vo = L_r \frac{\mathrm{d}i_{Lr}(t)}{\mathrm{d}t} + nV_{Cc} + v_{C1}(t), \tag{5}$$

$$i_{Lr}(t) = C_1 \frac{\mathrm{d}v_{C1}(t)}{\mathrm{d}t}. \tag{6}$$

Also, the initial condition is as follows

$$v_{C1} = -nV_{C_c} + \left(\frac{V_o}{2} + \Delta V_{C_1} + nV_{C_c}\right) \times \cos\left(\frac{2\pi}{f} D\right), \tag{7}$$

$$i_{Lr}(0) = 0 . \tag{8}$$

Mode 3 $(t_2, t_3 = T_s/2)$**:** At time t_2, S_1 and S_4 are turned off. In S_4 case, it turns off with ZVS since i_{L2} flows through D_{S4}. Diode D_2 is in forwarding bias. Diode D_2 current i_{D1} continues to flow in the same direction.

Mode 4 $(t_3 = T_s/2, t_4)$**:** At time t_3, the switches S_2 and S_3 turn on. Especially, S_3 is turned on with ZVS because D_{S3} has been conducted in Mode 3. Diode D_2 current i_{D2} continues to flow in the same direction as before until it gets to zero. As a result, the i_{L1} decreases linearly as

$$i_{L1}(t) = i_{L1}(t_3) - \frac{V_{Cc} - V_{in}}{L_1}(t - t_3) \tag{9}$$

and i_{L2} increases linearly as

$$i_{L2}(t) = i_{L2}(t_3) + \frac{V_{in}}{L_2}(t_3) . \tag{10}$$

Mode 5 (t_4, t_5)**:** During this time interval, Diode D_1 is in forward-biased condition, and Diode D_2 is in reversed-biased condition. i_{L1} decreases continuously as in (9), and i_{L2} increases continuously as in (10). In this mode, capacitor C_1 charges, and C_2 begins discharging. Capacitor C_1 forms an *RC* first-order circuit with zero input value.

Mode 6 $(t_5, t_6 = T)$**:** In this mode, S_2 and S_3 are turned off. In S_3 case, it turns off with ZVS since i_{L1} flows through D_{S3}. Diode D_1 is in forwarding bias. Diode D_1 current i_{D1} continues to flow in the same direction.

Fig. 2 illustrates the operating modes of the proposed converter during each time interval.

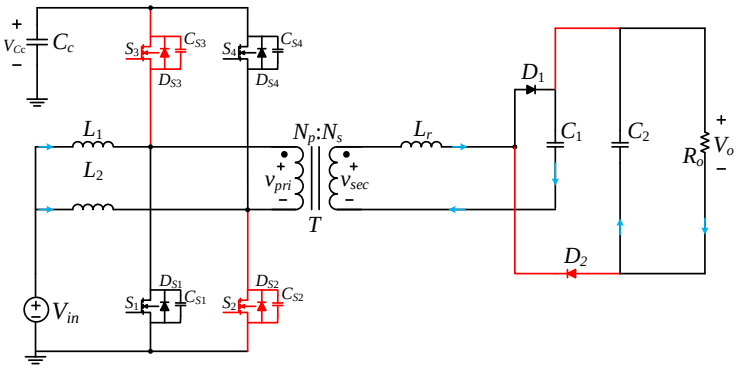

Fig. 2a – *The operation Mode 1* (t_0, t_1) *of the proposed converter.*

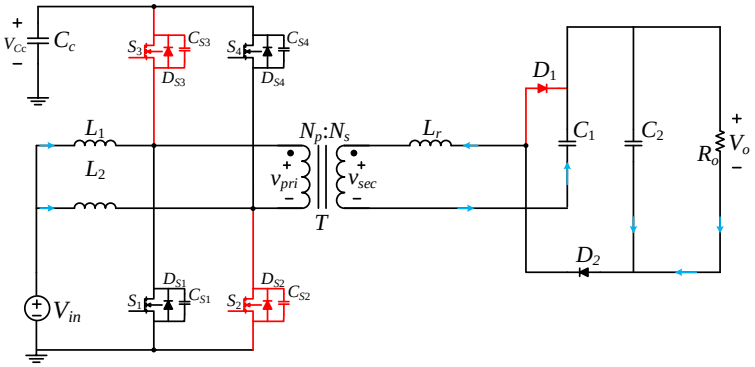

Fig. 2b – *The operation Mode 2* (t_1, t_2) *of the proposed converter.*

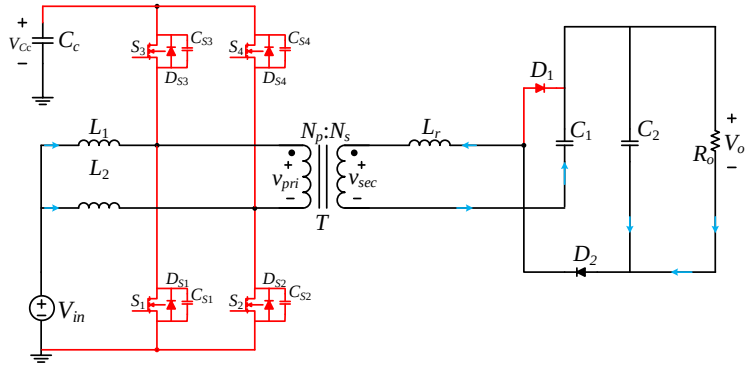

Fig. 2c – *The operation Mode 3* (t_2, $t_3 = T_s/2$) *of the proposed converter.*

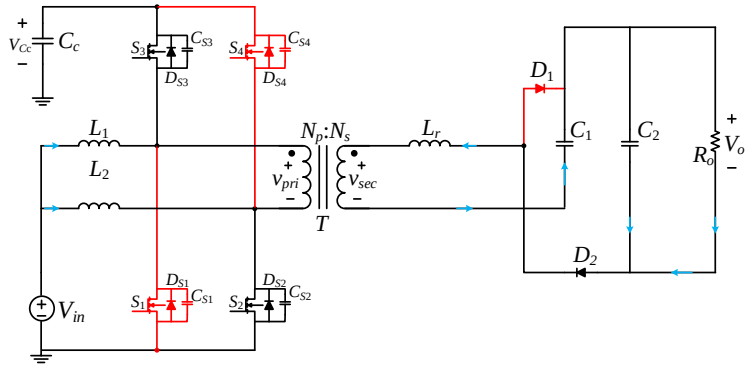

Fig. 2d – *The operation Mode 4* ($t_3 = T_s/2$, t_4) *of the proposed converter.*

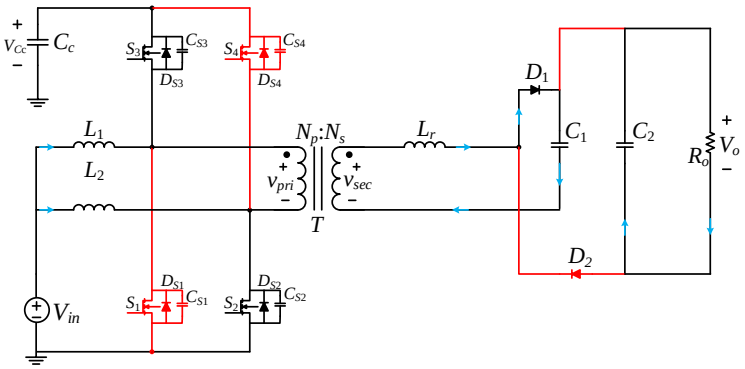

Fig. 2e – *The operation Mode 5* (t_4, t_5) *of the proposed converter.*

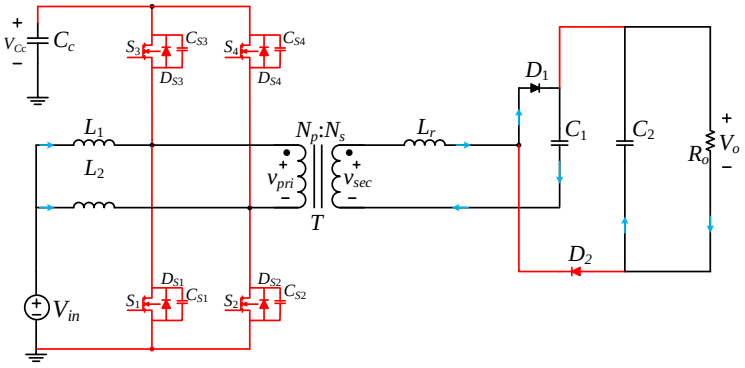

Fig. 2f – *The operation Mode 6* (t_5, $t_6 = T$) *of the proposed converter.*

Applying volt-second balance for the voltage across the inductor, the voltage gain of the proposed converter can be calculated as follows (the quality factor is considered 1):

$$\begin{cases} G = \dfrac{V_o}{V_i} = 4n\dfrac{A + B + \sqrt{(1-4B)A^2 + 6AB + B^2}}{2B(1-A)}, \\ A = 1 - \cos\left(\dfrac{2\pi}{f}D\right), \quad B = \dfrac{\pi Q}{2f}. \end{cases} \tag{11}$$

The main waveforms of several components of the proposed converter in CCM operation are shown in Fig. 3.

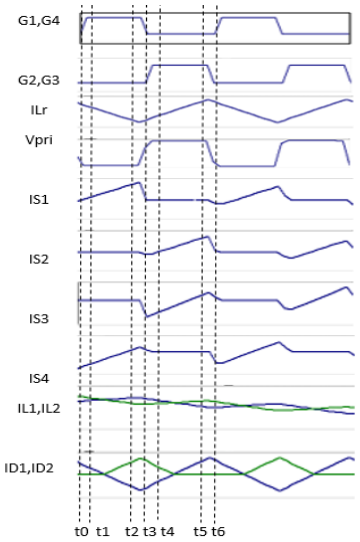

Fig. 3 – *The main waveforms of the proposed converter in CCM.*

4 Comparison Study

A Comparison between the proposed topology and some resonant converters is illustrated in **Table 1**.

Table 1
Comparison between some resonant converters and the proposed method.

	[9]	[10]	[13]	[19]	proposed
Efficiency [%]	94.5	86	95.7	95	95.8
Input current ripple [%]	2	38	35	48	8.4
No. of components	11	17	9	13	12
Output power	130	200	400	60	137
Degree of utilization	1	0.2	1	1	1
Losses	0.055 Pin	0.14 Pin	0.04 Pin	0.05 Pin	0.04 Pin
Frequency	100 kHz	50 kHz	50kHZ	100 kHz	50 kHz
Cost [$]	18.5	25	20	20	20

The converter proposed in [14] employs the secondary side resonance on the active clamp flyback converter to reduce root-mean-square (RMS) current values to enhance the performance of the synchronous rectifier [13]. The study conducted in [14] uses fewer semiconductor devices in which power is transferred to the output once the main switch becomes off. The dual series resonant converter requires fewer switching elements at the expense of overall voltage

gain. In addition, the voltages of resonant capacitors are not balanced. Compared to [19], the proposed converter requires fewer devices and attains voltage balance of resonant capacitors while achieving higher voltage gain. The calculated efficiency in [13] is less than that of the proposed converter at the heavy load. However, the efficiency in [13] is more than the proposed converter efficiency at light loads since the reverse recovery in [13] does not happen at these loads.

The main drawback of the current-fed interleaved converter discussed in [8] is that it necessitates the use of a great number of devices. The half-bridge current-fed converter in [11] demands fewer devices than the one in [8] but has a higher input current ripple. To overcome the problem, a circuit was developed for renewable energy applications at the expense of more elements and sophisticated control [20]. The voltage gain of the converters is depicted in Fig. 4a. The figure displays that the proposed converter has a higher gain than most similar converters. The proposed circuit can have high efficiency and high voltage gain even at low input voltages. Fig. 4b depicts converter efficiency versus input current ripple for several topologies.

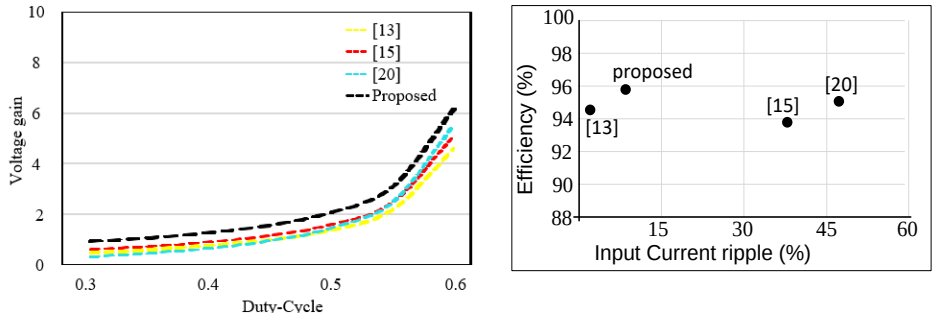

(a) (b)

Fig. 4 – *Comparison of the proposed converter with the other similar converters:* (a) *the voltage gains and duty-cycle;* (b) *the input current ripple and efficiency.*

5 Simulation Results

The proposed converter is simulated in PSCAD/EMTDC to verify the theoretical analysis and performance validity. The components' specifications of the simulation results are provided in **Table 2**.

Fig. 5 shows the voltage value of the capacitors C_c, C_1, and C_o, respectively. Fig. 5a illustrates the voltage value of capacitor C_c, approximately 78 V. Figs. 5b and 5c show the voltage values of capacitors C_1 and C_2, respectively, the former about 91 V and the latter 182 V. Fig. 6a shows the inductors L_1 and L_2 current waveform. The figure shows that the inductor's currents are similar with a 180° shift phase. The maximum value of the current of these inductors is equal to 6.13A. Fig. 6b illustrates the current waveform of the inductor L_r. Fig. 6c displays

the ripple percent of the input current of the proposed converter is low. The input current tolerances are between 5.7 A and 6.20 A.

Table 2

The characteristics of the proposed converter.

Input voltage	40 V
Switching frequency	50 kHz
All inductors	60 µH
All capacitors of voltage multiplier units	22 µF
Output capacitor C_o	220 µF
Output resistance R	241 Ω

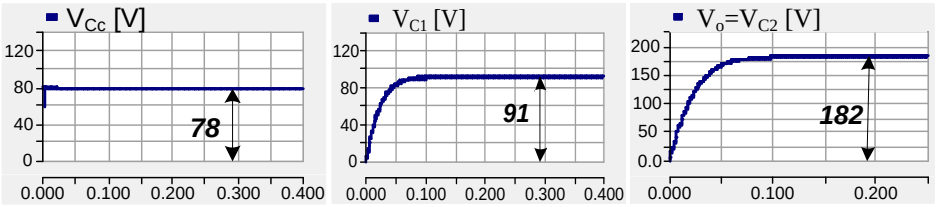

(a) (b) (c)

Fig. 5 – *The voltage of the capacitors:* (a) *voltage of capacitor* C_c*;* (b) *voltage of capacitor* C_1*;* (c) *voltage of capacitor* C_2 (V_o).

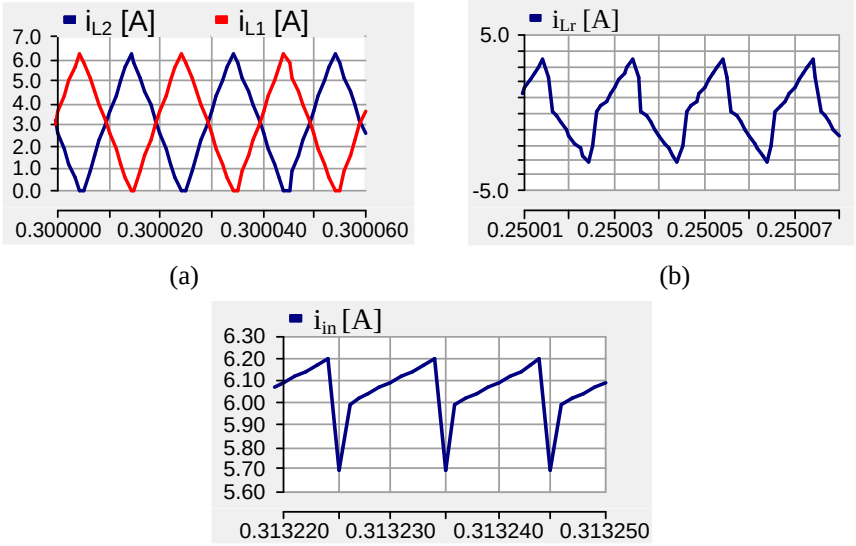

(a) (b)

(c)

Fig. 6 – *The currents of the inductors* L_1, L_2, L_r, *and the input current:* (a) *current of inductors* L_1, L_2*;* (b) *current of inductor* L_r*;* (c) *input current.*

Fig. 7a shows the current waveforms of the diodes D_1, D_2. Figs. 7b and 7c illustrate the current waveforms of the switches S_1 and S_4, respectively. As Figs. 7a and 7b indicate the power switch S_1 and S_4 are turned on in ZCS condition. As a result, the overall efficiency of the proposed circuit is increased. The voltage stress over S_4 is shown in Fig. 7d. According to the figure, the maximum voltage stress is about 78 V.

Comparing all of the fore-mention items with each other, it becomes conspicuous that the proposed converter is a suitable candidate for renewable resources due to its low input current ripple, high voltage gain, lower switching losses (with ZCS condition), and high efficiency. Renewable resources like photovoltaic systems have about 15-50 V panels with low output voltage. So, a high step-up dc-dc converter is required to boost and adjust the low voltage of a panel to the high voltage of the DC bus, which would be connected to an AC voltage through an inverter to the load or grid, as shown in Fig. 8.

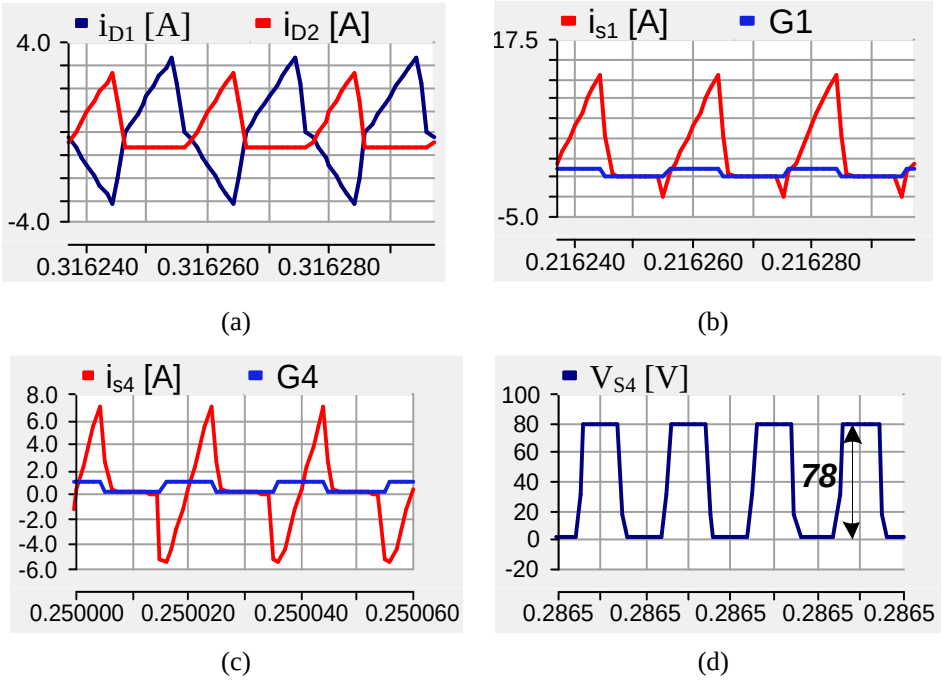

Fig. 7 – *The current and voltage waveforms of the semiconductors:* (a) *the currents of the diodes D_1 and D_2;* (b) *the current of the switch S_1;* (c) *the current of the switch S_4;* (d) *the voltage stress across the switch S_4.*

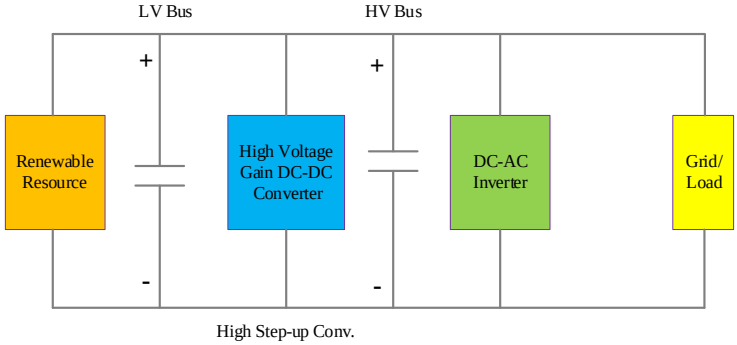

Fig. 8 – *Schematic of a renewable resource using the high voltage gain resonant DC-DC converter.*

6 Conclusion

In the present study, a novel DC-DC converter based on the resonant switched-capacitor (RSC) with a high voltage gain was examined, and it proved to be suitable for renewable energy resource applications. The resonant situation of the circuit provided the soft-switching mechanism. Hence, the switching losses were minimal in both ON and OFF conditions, and the power density of the proposed converter could be enhanced by increasing the switching frequency. It was shown that by using a variable switching-frequency control, the proposed converter would continuously operate even at the critical conduction mode. Employing the resonance mechanism, the proposed converter reduced the turn-on loss of the switching and decreased the reverse-recovery losses of the rectifying diodes. The switching operation on the secondary side of the proposed circuit resulted in the higher achieved voltage gain and fewer components. The proposed converter operation analysis was presented, together with some design points.

7 References

[1] N. Sifakis, S. Konidakis, T. Tsoutsos: Hybrid Renewable Energy System Optimum Design and Smart Dispatch for Nearly Zero Energy Ports, Journal of Cleaner Production, Vol. 310, August 2021, pp. 1 – 15.

[2] J. Huang, X. Zhang, B. Zhao: Simplified Resonant Parameter Design of the Asymmetrical CLLC-Type DC Transformer in the Renewable Energy System via Semi-Artificial Intelligent Optimal Scheme, IEEE Transactions on Power Electronics, Vol. 35, No. 2, February 2020, pp. 1548 – 1562.

[3] M. Shirzadi, S. M. Dehghan, E. Najafi: High-Step-Up Enhanced Super-Lift Converter, IET Power Electronics, Vol. 13, No. 17, December 2020, pp. 3890 – 3899.

[4] E. Najafi, H. Shojaeian, M. Kashi: A High Gain Step Up Converter for Solar Applications based on PSOL Topology, Journal of Solar Energy Research, Vol. 4, No. 3, October 2019, pp. 180 – 187.

[5] A. Mirzaei, M. Rezvanyvardom, E. Najafi: A Fully Soft Switched High Step-Up SEPIC-Boost DC-DC Converter with One Auxiliary Switch, International Journal of Circuit Theory and Applications, Vol. 47, No. 3, March 2019, pp. 427 – 444.

[6] S. Mohsen Salehi, S. Hasanzadeh, H. Shojaeian: A Dual Switch/Inductor Isolated High Voltage Gain based on Voltage Lift, Proceedings of the 12th Power Electronics, Drive Systems, and Technologies Conference (PEDSTC), Tabriz, Iran, February 2021, pp. 1 – 5.

[7] C. C. Kuo, J. J. Lee, Y. H. He, J. Y. Wu, K. H. Chen, Y. H. Lin, S. R. Lin, T. Y. Tsai: A Dynamic Resonant Period Control Technique for Fast and Zero Voltage Switching in GaN-Based Active Clamp Flyback Converters, IEEE Transactions on Power Electronics, Vol. 36, No. 3, March 2021, pp. 3323 – 3334.

[8] R. Sun, Y. C. Liang, Y.- C. Yeo, C. Zhao, W. Chen, B. Zhang: All-GaN Power Integration: Devices to Functional Subcircuits and Converter ICs, IEEE Journal of Emerging and Selected Topics in Power Electronics, Vol. 8, No. 1, March 2020, pp. 31 – 41.

[9] J. W. Yang, H. L. Do: Bridgeless SEPIC Converter with a Ripple-Free Input Current, IEEE Transactions on Power Electronics, Vol. 28, No. 7, July 2013, pp. 3388 – 3394.

[10] D. Sha, Y. Xu, J. Zhang, Y. Yan: Current-Fed Hybrid Dual Active Bridge DC-DC Converter for a Fuel Cell Power Conditioning System with Reduced Input Current Ripple, IEEE Transactions on Industrial Electronics, Vol. 64, No. 8, August 2017, pp. 6628 – 6638.

[11] J. Hassan, C. Bai, H. Seok, J.- W. Lim, S.- H. Ahn, M. Kim: Highly Efficient Current-Fed Half-Bridge Resonant Converter for Pulse Power Applications, IEEE Transactions on Power Electronics, Vol. 37, No. 3, March 2022, pp. 3192 – 3204.

[12] Y. Huang, S. Xiong, S.- C. Tan, S. Y. Hui: Nonisolated Harmonics-Boosted Resonant DC/DC Converter with High-Step-Up Gain, IEEE Transactions on Power Electronics, Vol. 33, No. 9, September 2018, pp. 7770 – 7781.

[13] S. Son, O. A. Montes, A. Junyent-Ferre, M. Kim: High Step-Up Resonant DC/DC Converter with Balanced Capacitor Voltage for Distributed Generation Systems, IEEE Transactions on Power Electronics, Vol. 34, No. 5, May 2019, pp. 4375 – 4387.

[14] M. Dalla Vecchia, G. Van den Broeck, S. Ravyts, J. Tant, J. Driesen: A Family of DC–DC Converters with High Step-Down Voltage Capability based on the Valley-Fill Switched Capacitor Principle, IEEE Transactions on Industrial Electronics, Vol. 68, No. 7, July 2021, pp. 5810 – 5820.

[15] H. Shojaeian, S. Hasanzadeh, S. M. Salehi: A Single Switch High Voltage Gain DC-DC Converter based on Coupled Inductor and Switched-Capacitor for Renewable Energy Systems, Proceedings of the 12th Power Electronics, Drive Systems, and Technologies Conference (PEDSTC), Tabriz, Iran, February 2021, pp. 1 – 6.

[16] S. M. Salehi, S. M. Dehghan, S. Hasanzadeh: Interleaved-Input Series-Output Ultra-High Voltage Gain DC-DC Converter, IEEE Transactions on Power Electronics, Vol. 34, No. 4, April 2019, pp. 3397 – 3406.

[17] R. Beiranvand, S. H. Sangani: A Family of Interleaved High Step-Up DC-DC Converters by Integrating a Voltage Multiplier and an Active Clamp Circuits, IEEE Transactions on Power Electronics, 2022.

[18] H. Shojaeian, S. Hasanzadeh, S. M. Salehi: A Single Switch High Voltage Gain DC-DC Converter based on Coupled Inductor and Switched-Capacitor for Renewable Energy Systems, Proceedings of the 12th Power Electronics, Drive Systems, and Technologies Conference (PEDSTC), Tabriz, Iran, February 2021, pp. 1 – 6.

[19] M. M. Ghahderijani, M. Castilla, A. Momeneh, J. T. Miret, L. G. de Vicuna: Frequency-Modulation Control of a DC/DC Current-Source Parallel-Resonant Converter, IEEE Transactions on Industrial Electronics, Vol. 64, No. 7, July 2017, pp. 5392 – 5402.

[20] H. Seok, B. Han, B.- H. Kwon, M. Kim: High Step-Up Resonant DC-DC Converter with Ripple-Free Input Current for Renewable Energy Systems, IEEE Transactions on Industrial Electronics, Vol. 65, No. 11, November 2018, pp. 8543 – 8552.